

Holographic Entanglement of Purification from Conformal Field Theories

Pawel Caputa^a, Masamichi Miyaji^a,
Tadashi Takayanagi^{a,b} and Koji Umemoto^a

^a*Center for Gravitational Physics,
Yukawa Institute for Theoretical Physics, Kyoto University,
Kitashirakawa Oiwakecho, Sakyo-ku,
Kyoto 606-8502, Japan and*

^b*Kavli Institute for the Physics and Mathematics of the Universe (WPI),
University of Tokyo, Kashiwa, Chiba 277-8582, Japan*

(Dated: December 14, 2018)

We explore a conformal field theoretic interpretation of the holographic entanglement of purification, which is defined as the minimal area of entanglement wedge cross section. We argue that in AdS₃/CFT₂, the holographic entanglement of purification agrees with the entanglement entropy for a purified state, obtained from a special Weyl transformation, called path-integral optimizations. By definition, this special purified state has the minimal path-integral complexity. We confirm this claim in several examples.

1. Introduction

Quantum entanglement provides us a key to understand how gravity emerges from field theories. This is manifest in the Anti de-Sitter space(AdS)/conformal field theory(CFT) correspondence (or holography) [1]. In AdS/CFT, the entanglement entropy, the unique measure of quantum entanglement for pure states, is computed as a minimal area in AdS [2, 3].

For mixed states, entanglement entropy can measure neither quantum entanglement nor correlations between two subsystems. Recently, it was conjectured that a quantity called entanglement of purification [4], which is a good measure of total correlations, has a simple geometric interpretation in AdS/CFT, called the holographic entanglement of purification [5, 6]. This quantity is a natural extension of entanglement entropy for mixed states. An extension to multi-partite correlations is also given in [7].

The entanglement of purification (EoP), written as $E_P(\rho_{AB})$, is a measure of correlations between two subsystems A and B for a mixed state ρ_{AB} and is defined as follows [4]. Consider a purification of ρ_{AB} , given by $|\Psi\rangle_{A\bar{A}B\bar{B}}$, by enlarging the Hilbert space as $\mathcal{H}_A \otimes \mathcal{H}_B \rightarrow \mathcal{H}_A \otimes \mathcal{H}_B \otimes \mathcal{H}_{\bar{A}} \otimes \mathcal{H}_{\bar{B}}$ such that

$$\rho_{AB} = \text{Tr}_{\bar{A}\bar{B}} [|\Psi\rangle_{A\bar{A}B\bar{B}}\langle\Psi|_{A\bar{A}B\bar{B}}]. \quad (1)$$

Among infinitely many different choices of the purifications $|\Psi\rangle_{A\bar{A}B\bar{B}}$, the EoP is defined by minimizing the entanglement entropy $S_{A\bar{A}} = -\text{Tr}[\rho_{A\bar{A}} \log \rho_{A\bar{A}}]$ as

$$E_P(\rho_{AB}) = \min_{|\Psi\rangle_{A\bar{A}B\bar{B}}} [S_{A\bar{A}}]. \quad (2)$$

The holographic entanglement of purification (HEoP) $E_W(\rho_{AB})$ is defined by the area of the minimal cross section of entanglement wedge, denoted by Σ_{AB}^{min} :

$$E_W(\rho_{AB}) = \frac{A(\Sigma_{AB}^{\text{min}})}{4G_N}, \quad (3)$$

and the equality $E_W(\rho_{AB}) = E_P(\rho_{AB})$ was conjectured in [5, 6] based on quantum information theoretic properties. In this paper, we focus on static backgrounds and always take a canonical time slice in the AdS.

The entanglement wedge is the region inside the AdS which is dual to the density matrix ρ_{AB} [8–10]. Therefore, the HEoP (3) is quite fundamental to understand how the geometry in gravity corresponds to density matrices in CFTs. It also has an important meaning in the bit threads interpretation of AdS/CFT [11–14].

Nevertheless, direct comparisons between the HEoP and EoP have not been done so far mainly because the minimization procedure in (2) is very hard in quantum field theories. Refer to [6, 15, 16] for numerical lattice calculations of EoP in free field theories. Also in [17–19], connections between $E_W(\rho_{AB})$ and quantities other than the EoP have been proposed. For other recent progresses on the HEoP, refer to [20–32].

In this letter, we would like to present a direct comparison between the HEoP $E_W(\rho_{AB})$ and the entanglement entropy $S_{A\bar{A}}$ for a special class of purification $|\Psi\rangle_{A\bar{A}B\bar{B}}$, obtained by the path-integral optimization [33, 34]. We will focus on several examples in AdS₃/CFT₂ and will find both quantities always agree with each other in the regime of validity of our computations.

2. Path-Integral Optimization

Consider a two dimensional (2D) CFT on a Euclidean flat space R^2 , which is described by the complex coordinate $(w, \bar{w}) = (\xi + i\tau, \xi - i\tau)$ with the metric

$$ds^2 = dwd\bar{w} = d\tau^2 + d\xi^2. \quad (4)$$

The theory is invariant under the Weyl transformation of the metric:

$$ds^2 = e^{2\phi(\tau, \xi)}(d\tau^2 + d\xi^2), \quad (5)$$

where $\phi(\tau, \xi)$ is any function.

The path-integral optimization [33] is a special choice of Weyl transformation which (i) preserves the quantum state $|\Psi\rangle$ at a particular time $\tau = \tau_0$ and (ii) minimizes the path-integral complexity $C_L[\phi]$ (defined below).

Since the wave functional of $|\Psi\rangle$ can be computed by the Euclidean path-integral on the lower half plane $-\infty < \tau \leq \tau_0$, the first condition (i) is given by the boundary condition

$$e^{2\phi(\tau_0, \xi)} = 1. \quad (6)$$

The path-integral complexity is defined by the Liouville action

$$C_L[\phi] = \frac{c}{24\pi} \int_{-\infty}^{\tau_0} d\tau \int_{-\infty}^{\infty} d\xi \left[(\partial_\tau \phi)^2 + (\partial_\xi \phi)^2 + \frac{e^{2\phi}}{\epsilon^2} \right], \quad (7)$$

where ϵ is the UV cut off or equally lattice spacing and c is the central charge. The reason why we identify $C_L[\phi]$ with the complexity in path-integrations is because the path-integral measure is proportional to $e^{C_L[\phi]}$ due to the conformal anomaly [35]. This quantity $C_L[\phi]$ provides a field theoretic counterpart of holographic complexity [36] as explained in [37].

In this argument, we consider the discretization of path-integral such that each cell has the area ϵ^2 . The original flat metric (4) corresponds to a square lattice with lattice spacing $\Delta\xi = \Delta\tau = \epsilon$. The optimization which changes the metric such that $e^{2\phi} \leq 1$ means coarse-graining lattice sites such that $\Delta\xi = \Delta\tau = \epsilon \cdot e^{-\phi}$.

The minimization of $C_L[\phi]$ can be found by solving the Liouville equation $(\partial_\tau^2 + \partial_\xi^2)\phi = e^{2\phi}/\epsilon^2$. Choosing $\tau_0 = -\epsilon$ using the time translational symmetry, we find the solution which satisfies the condition (6)

$$e^{2\phi} = \frac{\epsilon^2}{\tau^2}. \quad (8)$$

This describes a hyperbolic space H_2 . Note that in [33] we had $e^{2\phi} = 1/z^2$ because we defined $z = -\epsilon$ with the rescaling $e^\phi \rightarrow \epsilon \cdot e^\phi$. This is the simplest example of the path-integral optimization. Even though we optimized a pure state $|\Psi\rangle$, it is straightforward to extend the formulation such that we optimize a given mixed state density matrix.

3. Optimization of Single Interval

Consider the case where the subsystem $AB(\equiv A \cup B)$ is given by a single interval in a vacuum. We parameterize the subsystem A and B as follows:

$$A = [a, p], \quad B = [p, b], \quad (-\infty < a < p < b < \infty), \quad (9)$$

where they share the point P given by $y = p$. The reduced density matrix ρ_{AB} is given by the Euclidean path-integral over a complex plane with a slit along AB , whose coordinate is denoted by y . Next we consider a purification $|\Psi\rangle_{A\tilde{A}B\tilde{B}}$ of ρ_{AB} by introducing the subsystem \tilde{A}

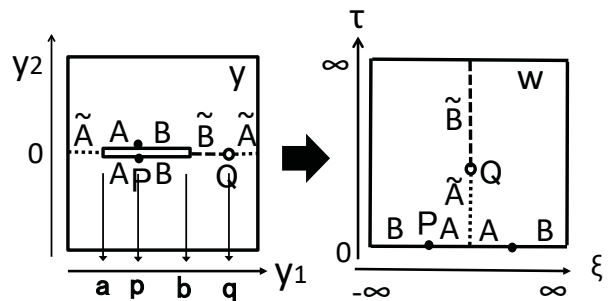


FIG. 1. Conformal transformation between a complex plane with one slit and an upper half plane.

and \tilde{B} as in Fig.1 such that they share the point Q parameterized by $y = q$.

The original definition of EoP is the minimum of $S_{A\tilde{A}}$ against any purifications (2). Here we would like to restrict to a class of purification which is realized by the Weyl transformation (5) and focus on the one given by the path-integral optimization (i.e. the one which minimizes $C_L[\phi]$). The purification condition (1) is equivalent to the requirement (6).

To find the optimization, let us map the y -space into an upper half-plane (w -plane) by

$$w = \sqrt{\frac{y-a}{b-y}}. \quad (10)$$

The point P and Q are mapped into $w_P = -\sqrt{\frac{p-a}{b-p}}$ and $w_Q = i\sqrt{\frac{q-a}{q-b}}$.

Since the path-integral optimization on the upper half plane is given by the hyperbolic space (8), the final optimized metric reads

$$ds^2 = \frac{\epsilon^2}{\tau^2} \cdot dwd\bar{w} = \frac{\epsilon^2}{\tau^2} \cdot \frac{(b-a)^2}{4|b-y|^3|y-a|} \cdot dyd\bar{y} \equiv e^{2\tilde{\phi}} \cdot dyd\bar{y}. \quad (11)$$

The coordinate τ takes values in the range $-\infty < \tau < -\delta_1$, where $\delta_1(> 0)$ is an appropriate cut off so that we maintain the condition (1). However, the detail of this regularization is not important in the coming calculations and refer to the appendix A for more explanations. In this setup, we have $e^{2\tilde{\phi}_P} = 1$, which follows from the condition (4), and we find $e^{2\tilde{\phi}_Q} = \frac{\epsilon^2(b-a)^2}{4(q-a)^2(q-b)^2}$, where $\tilde{\phi}_P$ and $\tilde{\phi}_Q$ are the value of $\tilde{\phi}$ at P and Q .

The entanglement entropy $S_{A\tilde{A}} = S_{B\tilde{B}}$ is found to be

$$\begin{aligned} S_{A\tilde{A}} &= \frac{c}{3} \log \left(\frac{q-p}{\epsilon} \right) + \frac{c}{6} \tilde{\phi}_P + \frac{c}{6} \tilde{\phi}_Q \\ &= \frac{c}{6} \log \left[\frac{(b-a)(q-p)^2}{2\epsilon(q-a)(q-b)} \right], \end{aligned} \quad (12)$$

where in the first line we performed a scale transformation of the standard formula of [38]. Remember that the

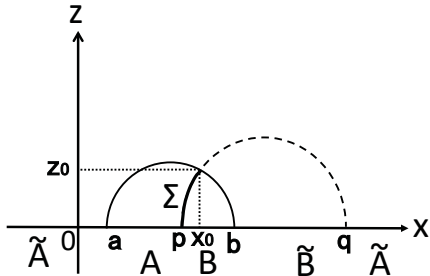


FIG. 2. Calculation of Holographic EoP. The length of Σ (thick curve in the above picture) multiplied by $\frac{1}{4G_N} = \frac{c}{6}$ gives the holographic EoP (3).

entanglement entropy can be found from the two point function of twist operators in the replica method and this transforms in a standard way under the Weyl transformation. Then we minimize $S_{A\bar{A}}$ with respect to q , leading to

$$S_{AA}^{min} = \frac{c}{6} \log \left[\frac{2(p-a)(b-p)}{\epsilon(b-a)} \right], \quad (13)$$

$$\text{at } q = \frac{2ab - (a+b)p}{a+b-2p}. \quad (14)$$

The holographic EoP is computed from the length of the entanglement wedge cross section Σ_{AB}^{min} in the hyperbolic space $ds^2 = (dx^2 + dz^2)/z^2$, which is a time slice of Poincare AdS₃. The geodesic curve Σ_{AB}^{min} is a part of a circle which connects $P : (x, z) = (p, \epsilon)$ and $Q : (x, z) = (q, \epsilon)$, as depicted in Fig.2. The minimal length condition requires that Σ_{AB}^{min} is perpendicular to the circle $(x - \frac{a+b}{2})^2 + z^2 = \frac{(b-a)^2}{4}$ at their intersection point $(x, z) = (x_0, z_0)$. This fixes the value of q as (14) and we obtain $x_0 = \frac{pq-ab}{p+q-(a+b)}$ and $z_0 = \sqrt{\frac{(b-a)^2}{4} - (x_0 - \frac{a+b}{2})^2}$. Its length $A(\Sigma_{AB}^{min})$ is computed as

$$\frac{q-p}{2} \int_{\epsilon}^{z_0} \frac{dz}{z \sqrt{\frac{(q-p)^2}{4} - z^2}} = \log \left[\frac{2(p-a)(p-b)}{\epsilon(b-a)} \right].$$

Thus the holographic EoP (3) perfectly matches with (13).

It is straightforward to extend the above agreement between $E_W(\rho_{AB})$ and $S_{A\bar{A}}$ to the finite temperature case by performing a conformal transformation $y = e^{\frac{2\pi}{\beta}\zeta}$. Similarly, we can extend it to the finite size case.

4. Optimization of Double Intervals

As the second class of examples, we consider the case where the subsystems A and B are mutually disconnected intervals on an infinite line. Though we focus on the vacuum state in a two dimensional CFT below, it is straightforward to extend to the finite temperature setup by the conformal map $y = e^{\frac{2\pi}{\beta}\zeta}$ as before.

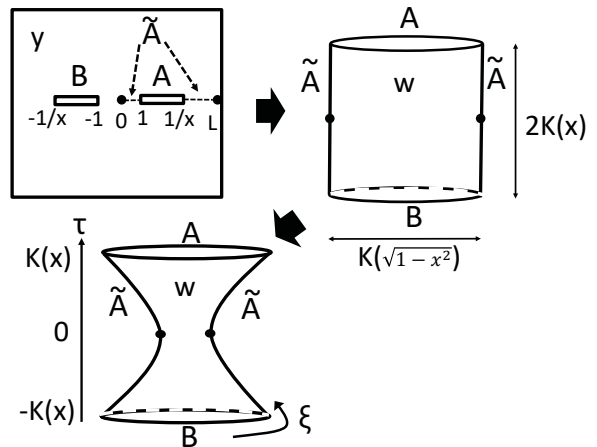


FIG. 3. Conformal map from complex plane with two cuts to a cylinder and its path-integral optimization.

The reduced density matrix ρ_{AB} is described by an Euclidean path-integral on the complex plane (y -plane) with two slits along A and B as in the upper left picture of Fig.3. Since ρ_{AB} depends only on the cross ratio η owing to the conformal invariance, without losing generality, we can fully parameterize the subsystem A and B as:

$$A = [1, 1/x], \quad B = [-1/x, -1], \quad (0 < x < 1). \quad (15)$$

The cross ratio is given by $\eta = (1-x)^2/4x$. We can choose the subsystem \tilde{A} and \tilde{B} which purify ρ_{AB} such that $A\tilde{A} = [0, L]$ and take the limit $L \rightarrow \infty$, owing to the reflection symmetry. We confirmed numerically that this reflection symmetry is not spontaneously broken.

The y -plane with two slits is mapped into a cylinder, which is described by the coordinate $w = \xi + i\tau$, as:

$$w = i \int_0^y d\tilde{y} \frac{1}{\sqrt{(1-\tilde{y}^2)(1-x^2\tilde{y}^2)}}, \quad (16)$$

as in the upper right of Fig.3.

Finally, we perform the path-integral optimization on a cylinder as in the lower picture of Fig.3. We obtain the optimized metric by solving the Liouville equation:

$$ds^2 = e^{2\phi} dw d\bar{w} = e^{2\tilde{\phi}} dy d\tilde{y}, \quad (17)$$

where

$$e^{2\phi} = \frac{\pi^2}{4K(x)^2} \cdot \frac{\epsilon^2}{\cos^2\left(\frac{\pi\tau}{2K(x)}\right)},$$

$$e^{2\tilde{\phi}} = e^{2\phi} \cdot \frac{1}{|(1-y^2)(1-x^2y^2)|^2}. \quad (18)$$

We introduced the elliptic function $K(x)$:

$$K(x) = \int_0^1 d\tilde{y} \frac{1}{\sqrt{(1-\tilde{y}^2)(1-x^2\tilde{y}^2)}}. \quad (19)$$

The coordinates τ takes values in the range:

$$-K(x) + \delta_2 \leq \tau \leq K(x) - \delta_2, \quad (20)$$

and ξ is periodically identified: $\xi \sim \xi + 2K(\sqrt{1-x^2})$. Here δ_2 is an infinitesimally small regularization parameter fixed by the condition (1). Again, the detail of δ_2 is not important in our calculations below and refer to appendix A for details. The boundary points of AA : $y = 0$ and $y = L(\rightarrow \infty)$ are mapped into the antipodal two points in the middle: $(\xi, \tau) = (0, 0)$ and $(\xi, \tau) = (K(\sqrt{1-x^2}), 0)$.

Now the entanglement entropy S_{AA}^{min} after the optimization can be computed as follows:

$$\begin{aligned} S_{AA}^{min} &= \frac{c}{3} \log \frac{L}{\epsilon} + \frac{c}{6} \tilde{\phi}|_{y=L} + \frac{c}{6} \tilde{\phi}|_{y=0} \\ &= \frac{c}{3} \log \frac{L}{\epsilon} + \frac{c}{6} \log \left[\frac{\pi\epsilon}{2L^2 x K(x)} \right] + \frac{c}{6} \log \left[\frac{\pi\epsilon}{2K(x)} \right] \\ &= -\frac{c}{6} \log x - \frac{c}{3} \log \left[\frac{2K(x)}{\pi} \right]. \end{aligned} \quad (21)$$

Since $K(x) \simeq \frac{\pi}{2} + \frac{\pi}{8}x^2 + \dots$ for $x \ll 1$, we have

$$S_{AA}^{min} = -\frac{c}{6} \log x + O(x^2). \quad (22)$$

We can compare this with the holographic EoP [5, 6]:

$$E_W(\rho_{AB}) = -\frac{c}{6} \log x, \quad (0 < x < 3 - 2\sqrt{2}). \quad (23)$$

For $3 - 2\sqrt{2} < x < 1$ we have $E_W(\rho_{AB}) = 0$ as the entanglement wedge gets disconnected.

It is also useful to note that the holographic mutual information (HMI) $I(A : B) = S_A + S_B - S_{AB}$ behaves

$$\frac{1}{2}I(A : B) = \frac{c}{6} \log z = \frac{c}{6} \log \frac{(1-x)^2}{4x} \quad (0 < x < 3 - 2\sqrt{2}), \quad (24)$$

while $I(A : B) = 0$ for $3 - 2\sqrt{2} < x < 1$. We plotted these quantities in Fig.4.

We notice that S_{AA}^{min} almost coincides with $E_W(\rho_{AB})$ for $0 < x < 3 - 2\sqrt{2}$ in the plot. However, one may worry that they deviate from each other at the order $O(x^2)$. Also, S_{AA}^{min} continuously decreases and becomes incorrectly negative as x gets larger. We would like to argue that our Weyl invariance (17) breaks down except for $x \ll 1$. This is because the length of minimal cross section of the optimized cylinder, given by $L_{cyl} = \frac{\pi\epsilon K(\sqrt{1-x^2})}{K(x)}$, is much greater than the cut off scale ϵ only if $x \ll 1$. If the size of manifold on which we path-integrate gets the same order of the lattice spacing ϵ , we cannot trust field theoretic properties of path-integrals, such as the Weyl invariance. Therefore, the result (21) is trustable only for $x \ll 1$ and in this range the equality $S_{AA}^{min} = E_W(\rho_{AB})$ is confirmed. Indeed, in the single interval case, where we found the perfect matching (13),

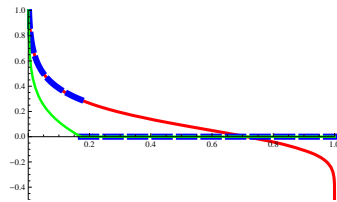


FIG. 4. Plots of HEoP (red), $I(A : B)/2$ (green) and S_{AA}^{min} (blue dashed) as a function of x . The first two get vanishing for $x > 3 - 2\sqrt{2}$. Note that the plot of S_{AA}^{min} is valid only when $x \ll 1$, where it coincides with HEoP.

the Weyl transformation is trustable for any values of a, b and p because we always have $L_{cyl} = \infty$.

It is also useful to note that at the holographic phase transition point $x = 3 - 2\sqrt{2}$ (or equally $\eta = 1$), the minimum cross section of the cylinder becomes $L_{cyl} = 2\pi\epsilon$. This indeed agrees with the point where a counterpart of confinement/deconfinement transition is expected in the path-integral optimization for holographic CFTs as argued in [33], though we cannot fully trust this argument because L_{cyl} gets as small as the lattice spacing ϵ .

5. Conclusions and Discussions

In this letter, for a given mixed state ρ_{AB} , we introduced a minimized entanglement entropy S_{AA}^{min} as follows. First we define a special purified state $|\Psi_{min}\rangle_{ABC}$ for ρ_{AB} by minimizing the path-integral complexity C_L (7). Then S_{AA}^{min} is given by taking the minimum of S_{AA} for the purified state $|\Psi_{min}\rangle_{ABC}$ among all possible decompositions of the ancilla space for purification $C = \tilde{A} \cup \tilde{B}$.

We analytically computed this quantity S_{AA}^{min} in several setups in two dimensional CFTs. Remarkably, we found that it matches with the area of the entanglement wedge cross section $E_W(\rho_{AB})$ in AdS, called the holographic entanglement of purification.

It is not obvious at present if our special purification is identical to the one which minimizes S_{AA} as in the original definition (2). However, we expect they are at least very close to each other because the former minimizes the path-integral complexity and thus efficiently compresses the sizes of \tilde{A} and \tilde{B} . In this sense, our result can be regarded as the first quantitative evidence for the holographic EoP conjecture [5, 6].

In the original argument [5], the equivalence between $E_W(\rho_{AB})$ and $E_P(\rho_{AB})$ was explained by assuming the surface/state duality [39], based on the conjectured relation between tensor networks [40, 41] and AdS/CFT [42]. In this argument, the minimization is taken only for quantum states with classical gravity duals. We would like to leave for future works the precise meaning of the minimum in the EoP (2) which correctly matches with $E_W(\rho_{AB})$. Higher dimensional generalizations are also an intriguing future problem.

Acknowledgements We thank Juan Maldacena, Brian Swingle, Kotaro Tamaoka and Guifre Vidal for useful conversations. MM and KU are supported by JSPS fellowships. PC and TT are supported by the Simons Foundation through the “It from Qubit” collaboration. PC is supported by JSPS Grant-in-Aid for Research Activity start-up 17H06787. MM is supported by JSPS Grant-in-Aid for JSPS Fellows No.16J08909. TT is supported by JSPS Grant-in-Aid for Scientific Research (A) No.16H02182 and by JSPS Grant-in-Aid for Challenging Research (Exploratory) 18K18766. TT is also supported by World Premier International Research Center Initiative (WPI Initiative) from the Japan Ministry of Education, Culture, Sports, Science and Technology (MEXT). KU is supported by JSPS Grant-in-Aid for JSPS Fellows No.18J2288 8.

-
- [1] J. M. Maldacena, “The Large N limit of superconformal field theories and supergravity,” *Int. J. Theor. Phys.* **38** (1999) 1113 [*Adv. Theor. Math. Phys.* **2** (1998) 231] [hep-th/9711200].
- [2] S. Ryu and T. Takayanagi, “Holographic derivation of entanglement entropy from AdS/CFT,” *Phys. Rev. Lett.* **96** (2006) 181602 [hep-th/0603001]; “Aspects of Holographic Entanglement Entropy,” *JHEP* **0608**, 045 (2006) [hep-th/0605073].
- [3] V. E. Hubeny, M. Rangamani and T. Takayanagi, “A Covariant holographic entanglement entropy proposal,” *JHEP* **0707** (2007) 062 [arXiv:0705.0016 [hep-th]].
- [4] B. M. Terhal, M. Horodecki, D. W. Leung and D. P. DiVincenzo, “The entanglement of purification,” *J. Math. Phys.* **43** (2002) 4286, doi:10.1063/1.1498001 [arXiv:quant-ph/0202044].
- [5] K. Umemoto and T. Takayanagi, “Entanglement of purification through holographic duality,” *Nature Phys.* **14** (2018) no.6, 573 doi:10.1038/s41567-018-0075-2 [arXiv:1708.09393 [hep-th]].
- [6] P. Nguyen, T. Devakul, M. G. Halbasch, M. P. Zaletel and B. Swingle, “Entanglement of purification: from spin chains to holography,” *JHEP* **1801** (2018) 098 doi:10.1007/JHEP01(2018)098 [arXiv:1709.07424 [hep-th]].
- [7] K. Umemoto and Y. Zhou, “Entanglement of Purification for Multipartite States and its Holographic Dual,” *JHEP* **1810** (2018) 152 doi:10.1007/JHEP10(2018)152 [arXiv:1805.02625 [hep-th]].
- [8] B. Czech, J. L. Karczmarek, F. Nogueira and M. Van Raamsdonk, “The Gravity Dual of a Density Matrix,” *Class. Quant. Grav.* **29** (2012) 155009 doi:10.1088/0264-9381/29/15/155009 [arXiv:1204.1330 [hep-th]].
- [9] A. C. Wall, “Maximin Surfaces, and the Strong Subadditivity of the Covariant Holographic Entanglement Entropy,” *Class. Quant. Grav.* **31** (2014) no.22, 225007 doi:10.1088/0264-9381/31/22/225007 [arXiv:1211.3494 [hep-th]].
- [10] M. Headrick, V. E. Hubeny, A. Lawrence and M. Rangamani, “Causality and holographic entanglement entropy,” *JHEP* **1412** (2014) 162 doi:10.1007/JHEP12(2014)162 [arXiv:1408.6300 [hep-th]].
- [11] M. Freedman and M. Headrick, “Bit threads and holographic entanglement,” *Commun. Math. Phys.* **352** (2017) no.1, 407 doi:10.1007/s00220-016-2796-3 [arXiv:1604.00354 [hep-th]].
- [12] V. E. Hubeny, “Bulk locality and cooperative flows,” arXiv:1808.05313 [hep-th].
- [13] S. X. Cui, P. Hayden, T. He, M. Headrick, B. Stoica and M. Walter, “Bit Threads and Holographic Monogamy,” arXiv:1808.05234 [hep-th].
- [14] C. A. Agon, J. de Boer and J. F. Pedraza, “Geometric Aspects of Holographic Bit Threads,” arXiv:1811.08879 [hep-th].
- [15] J. Hauschild, Johannes, E. Leviatan; J. Bardarson, E. Altman, M. Zaletel, F. Pollmann, “Finding purifications with minimal entanglement ,” eprint arXiv:1711.01288
- [16] A. Bhattacharyya, T. Takayanagi and K. Umemoto, “Entanglement of Purification in Free Scalar Field Theories,” *JHEP* **1804** (2018) 132 doi:10.1007/JHEP04(2018)132 [arXiv:1802.09545 [hep-th]].
- [17] H. Hirai, K. Tamaoka and T. Yokoya, “Towards Entanglement of Purification for Conformal Field Theories,” *PTEP* **2018** (2018) no.6, 063B03 doi:10.1093/ptep/pty063 [arXiv:1803.10539 [hep-th]].
- [18] J. Kudler-Flam and S. Ryu, “Entanglement negativity and minimal entanglement wedge cross sections in holographic theories,” arXiv:1808.00446 [hep-th].
- [19] K. Tamaoka, “Entanglement Wedge Cross Section from the Dual Density Matrix,” arXiv:1809.09109 [hep-th].
- [20] N. Bao and I. F. Halpern, “Holographic Inequalities and Entanglement of Purification,” *JHEP* **1803** (2018) 006 doi:10.1007/JHEP03(2018)006 [arXiv:1710.07643 [hep-th]].
- [21] D. Blanco, M. Leston and G. Perez-Nadal, “Gravity from entanglement for boundary subregions,” *JHEP* **0618** (2018) 130 doi:10.1007/JHEP06(2018)130 [arXiv:1803.01874 [hep-th]].
- [22] R. Espindola, A. Guijosa and J. F. Pedraza, “Entanglement Wedge Reconstruction and Entanglement of Purification,” *Eur. Phys. J. C* **78** (2018) no.8, 646 doi:10.1140/epjc/s10052-018-6140-2 [arXiv:1804.05855 [hep-th]].
- [23] N. Bao and I. F. Halpern, “Conditional and Multipartite Entanglements of Purification and Holography,” arXiv:1805.00476 [hep-th].
- [24] Y. Nomura, P. Rath and N. Salzetta, “Pulling the Boundary into the Bulk,” *Phys. Rev. D* **98** (2018) no.2, 026010 doi:10.1103/PhysRevD.98.026010 [arXiv:1805.00523 [hep-th]].
- [25] R. Abt, J. Erdmenger, M. Gerbershagen, C. M. Melby-Thompson and C. Northe, “Holographic Subregion Complexity from Kinematic Space,” arXiv:1805.10298 [hep-th].
- [26] A. May and E. Hijano, “The holographic entropy zoo,” *JHEP* **1810** (2018) 036 doi:10.1007/JHEP10(2018)036 [arXiv:1806.06077 [hep-th]].
- [27] Y. Chen, X. Dong, A. Lewkowycz and X. L. Qi, “Modular Flow as a Disentangler,” arXiv:1806.09622 [hep-th].
- [28] E. Caceres and M. L. Xiao, “Complexity-action of singular subregions,” arXiv:1809.09356 [hep-th].
- [29] J. C. Cresswell, I. T. Jardine and A. W. Peet, “Holographic relations for OPE blocks in excited states,”

- arXiv:1809.09107 [hep-th].
- [30] R. Q. Yang, C. Y. Zhang and W. M. Li, “Holographic entanglement of purification for thermofield double states and thermal quench,” arXiv:1810.00420 [hep-th].
- [31] N. Bao, A. Chatwin-Davies and G. N. Remmen, “Entanglement of Purification and Multiboundary Wormhole Geometries,” arXiv:1811.01983 [hep-th].
- [32] N. Bao, “Minimal Purifications, Wormhole Geometries, and the Complexity=Action Proposal,” arXiv:1811.03113 [hep-th].
- [33] P. Caputa, N. Kundu, M. Miyaji, T. Takayanagi and K. Watanabe, “Anti-de Sitter Space from Optimization of Path Integrals in Conformal Field Theories,” Phys. Rev. Lett. **119**, no. 7, 071602 (2017), [arXiv:1703.00456 [hep-th]]; “Liouville Action as Path-Integral Complexity: From Continuous Tensor Networks to AdS/CFT,” JHEP **1711** (2017) 097 [arXiv:1706.07056 [hep-th]].
- [34] A. Bhattacharyya, P. Caputa, S. R. Das, N. Kundu, M. Miyaji and T. Takayanagi, “Path-Integral Complexity for Perturbed CFTs,” JHEP **1807** (2018) 086 [arXiv:1804.01999 [hep-th]].
- [35] A. M. Polyakov, “Quantum Geometry of Bosonic Strings,” Phys. Lett. **103B** (1981) 207. doi:10.1016/0370-2693(81)90743-7
- [36] D. Stanford and L. Susskind, “Complexity and Shock Wave Geometries,” Phys. Rev. D **90** (2014) no.12, 126007 [arXiv:1406.2678 [hep-th]]; A. R. Brown, D. A. Roberts, L. Susskind, B. Swingle and Y. Zhao, “Holographic Complexity Equals Bulk Action?,” Phys. Rev. Lett. **116** (2016) no.19, 191301 doi:10.1103/PhysRevLett.116.191301 [arXiv:1509.07876 [hep-th]]; L. Lehner, R. C. Myers, E. Poisson and R. D. Sorkin, “Gravitational action with null boundaries,” Phys. Rev. D **94** (2016) no.8, 084046 [arXiv:1609.00207 [hep-th]].
- [37] T. Takayanagi, “Holographic Spacetimes as Quantum Circuits of Path-Integrations,” to appear in JHEP, arXiv:1808.09072 [hep-th].
- [38] C. Holzhey, F. Larsen and F. Wilczek, “Geometric and renormalized entropy in conformal field theory,” Nucl. Phys. B **424** (1994) 443 doi:10.1016/0550-3213(94)90402-2 [hep-th/9403108].
- [39] M. Miyaji and T. Takayanagi, “Surface/State Correspondence as a Generalized Holography,” PTEP **2015** (2015) 7, 073B03 doi:10.1093/ptep/ptv089 [arXiv:1503.03542 [hep-th]].
- [40] G. Vidal, “A class of quantum many-body states that can be efficiently simulated,” Phys. Rev. Lett. **101**, 110501 (2008), arXiv:quant-ph/0610099; “Entanglement renormalization,” Phys. Rev. Lett. **99**, 220405 (2007), arXiv:cond-mat/0512165.
- [41] G. Evenbly and G. Vidal, “Tensor Network Renormalization,” arXiv:1412.0732 [cond-mat.str-el], Phys. Rev. Lett. **115**, 180405 (2015); “Tensor network renormalization yields the multi-scale entanglement renormalization ansatz,” arXiv:1502.05385 [cond-mat.str-el], Phys. Rev. Lett. **115**, 200401 (2015).
- [42] B. Swingle, “Entanglement Renormalization and Holography,” Phys. Rev. D **86**, 065007 (2012), arXiv:0905.1317 [cond-mat.str-el].

APPENDIX A: DETAILS OF REGULARIZATION

In the path-integral optimization procedures, we encountered metrics $ds^2 = e^{2\phi} dy d\bar{y}$ which get divergent at the endpoints of AB such as (11) for the single interval and (18) for the double intervals. To maintain the boundary condition (1) on the slit AB , we actually need to shift the location of AB which is infinitesimal in the continuum limit $\epsilon \rightarrow 0$. This is equivalent to the cut off of the range of τ coordinate, denoted by δ_1 and δ_2 in the main context of this letter for the single and double interval, respectively (refer to e.g.(20) for the latter).

Let us study the detail of such a cut off by focusing on the double interval case, as the single interval case can be treated almost in the same way. The boundary condition (1) fixes the position dependent regularization δ_2 in (20) as

$$\delta_2 = \frac{\epsilon}{\sqrt{|(1-y^2)(1-x^2y^2)|}}. \quad (25)$$

One may worry that the relation (25) gets singular at the boundaries of A i.e. $y = 1$ and $y = 1/x$. However, this is not a problem as we can regularize the divergences at the two end points by eliminating infinitesimally small neighborhoods around them: $|y - 1| \leq \delta_0$ and $|y - 1/x| \leq \delta_0$ such that δ_2 is always small. Then we apply the same conformal map (16) to this regularized region. This is sketched in Fig.5. The regularization corresponds to eliminating the four edges of the cylinder in the w coordinate. Since we can take δ_0 infinitesimally small, these removed edges also get infinitesimally small. Because the twist operators are inserted at the end points of $A\bar{A}$, i.e. $w = 0$ and $w = K(\sqrt{1-x^2})$, this regularization procedure does not affect our calculation of $S_{A\bar{A}}^{min}$.

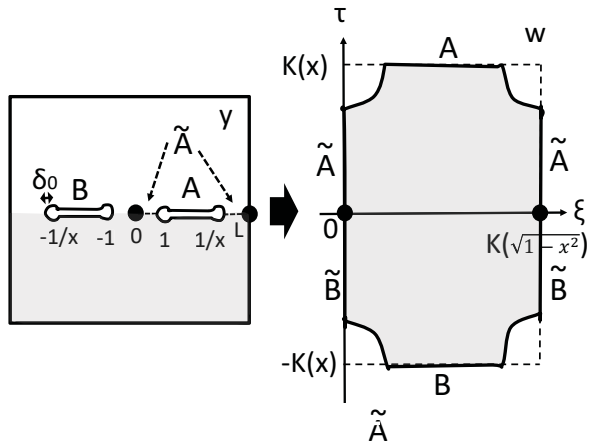


FIG. 5. A sketch of regularized conformal transformations, when AB are double intervals in the CFT vacuum. The grey colored region in the left is mapped to the same colored region in the right. The total plane with the two cuts on A and B eliminated, is mapped into two copies of the right picture, i.e. a cylinder.